

OMAE2014-24065

**EFFECT OF FLAP TYPE WAVE ENERGY CONVERTERS ON THE RESPONSE OF A
SEMI-SUBMERSIBLE WIND TURBINE IN OPERATIONAL CONDITIONS**

Constantine Michailides

Centre for Ships and Ocean Structures (CeSOS)
and Centre for Autonomous Marine Operations
and Systems (AMOS)
Norwegian University of Science and Technology
(NTNU)
Trondheim, Norway, 7491
Email: constantine.michailides@ntnu.no

Chenyu Luan

Centre for Ships and Ocean Structures (CeSOS)
and Centre for Autonomous Marine Operations and
Systems (AMOS), NTNU
Norwegian Research Centre for Offshore Wind
Technology, NTNU
Trondheim, Norway, 7491
Email: chenyu.luan@ntnu.no

Zhen Gao

CeSOS and AMOS
Norwegian University of Science and Technology
(NTNU)
Trondheim, Norway, 7491
Email: zhen.gao@ntnu.no

Torgeir Moan

CeSOS and AMOS, NTNU
Norwegian Research Centre for Offshore Wind
Technology
Trondheim, Norway, 7491
Email: torgeir.moan@ntnu.no

ABSTRACT

In the present paper the effect of flap type wave energy converters on the response of a floating semi-submersible wind turbine is investigated and reported. Two different layouts with regard to the number of rotating flaps that are utilized are considered and compared with the case of a pure floating semi-submersible wind turbine. Comparisons of response in terms of stability, motions and internal loads are made for selected environmental conditions. The combined operation of the rotating flaps results in an increase of the produced power without affecting significantly selected critical response quantities of the semi-submersible platform.

Keywords: Combined wind/wave concept, offshore wind turbine, wave energy converter, rotating flaps.

INTRODUCTION

Offshore wind energy is widely recognized as a useful source of renewable energy. Wind energy is also more mature than the other ocean renewable energy resources such as waves and tides mainly by using fixed-bottom concepts in shallow

water depths. For water depths larger than 100 m the use of floating wind turbines is considered as the most appropriate from a cost-benefit point of view; floating wind turbine concepts for deeper waters are still under development. Different floating support platform configurations are possible for use with offshore wind turbines such as tension leg platforms, spar-buoys and semi-submersibles [1]. Semi-submersible designs are commonly based to the OC4 DeepCWind semi-submersible wind turbine [2, 3], which is a three-column semi-submersible, supporting the 5 MW wind turbine on an additional central column. The columns are connected by braces. Alternatively, the columns of the semi-submersible platform can be connected by pontoons without any kind of braces ([4]).

In addition to offshore wind energy, ocean waves are an abundant and promising resource of alternative and clean energy with significant benefits compared to other forms of renewable ocean energy. The ocean wave energy has higher energy density, which enables the devices to extract more power from a smaller volume, limited negative environmental impact and more predictable energy ([5]). One major category of wave

energy converters is the rotating flaps ([6]). Usually those converters are oscillating about a fixed axis close to the sea bottom and as a result they are suitable for shallow and intermediate water depths. Hydrodynamic characteristics of such kind of devices are presented in [7] and [8]. In [9] and [10] the rotating flap is suggested to be fully submerged and to span vertically from the free surface to about one third of the water depth. According to the optimization study in [11] an elliptical section could be an optimal section for a fixed bottom rotating flap type wave energy converter. In order to convert the rotating motion of the flaps into useful power a rotation shaft connected with a hydraulic Power Take-Off (PTO) mechanism could be utilized. Up to now a limited number of rotating flaps are in operation.

It is therefore of interest to investigate possible combined systems for simultaneous extraction of wind and wave energy to possibly reduce the overall cost as well as to ensure an efficient use of the ocean space. Recently, EU research projects have been introduced to accelerate the development of combined offshore energy systems. The EU project MARINA Platform is dedicated to establish a set of equitable and transparent criteria for the evaluation of multi-purpose platforms for marine renewable energy as well as to develop design and analyses tools addressing those new multi-purpose renewable energy floating platforms ([12]). Under the scopes of the MARINA Platform project several researchers have studied combined concepts utilizing different floating support platforms ([13], [14] and [15]). Up to now, different types of wave energy converters have been considered for the proposed combined energy systems such as heaving buoys, oscillating water columns and overtopping devices. Among them, stands out the Spar-Torus Combination (STC) concept that consists of a spar platform that supports a wind turbine and reacts against a heaving torus wave energy device ([16], [17] and [18]). For all the combined concepts, it is important at the preliminary design stages to assure that the operation of the wave energy device will not affect the response of the floating support platform in an undesirable way.

The present paper deals with the behavior of combined semi-submersible wind turbine and rotating flap type wave energy converters. It is mentioned that the specific combined concept under investigation is proposed in the MARINA Platform project. The combined floating system consists of a semi-submersible floating platform with pontoons connecting the side columns to the central column at the bottom and two or three rotating flaps hinged at the pontoons of the semi-submersible as sketched in Fig. 1 through two rigid structural arms. The rotating flaps are fully submerged and the lower point of the rotating flap is 15 m above the pontoon of the semi-submersible platform. Modeling and analysis in the time-domain of the combined concept in a stochastic wind and wave environment are carried out using the coupled tool Simo/Riflex/AeroDyn [19]. Analysis is performed in order to examine the effect of utilizing two or three rotating flaps on the response of the proposed combined system as well as to

compare the response with that for the case that the semi-submersible support-platform does not contain any wave energy device and operates as a pure floating wind turbine. The response quantities that are compared are the motions of the support-platform, internal loads in the tower and blades of the wind turbine, fairlead tension of the mooring lines and (aggregate) produced power. The combined operation of the rotating flaps results in an increase of the produced power without affecting significantly selected critical response quantities of the semi-submersible platform. It should be mentioned that the design of the present combined concept is carried out by the Norwegian University of Science and Technology (NTNU) under the MARINA Platform project.

DESIGN CHARACTERISTICS AND DYNAMIC MODELING

The combined concept consists of: a) a semi-submersible floating platform with four columns (one central column and three side columns) and three pontoons connecting the side columns to the central column, b) a 5 MW wind turbine placed on the central column of the semi-submersible platform, c) two or alternatively three rotating flaps hinged at the pontoons of the semi-submersible through two rigid structural arms and linear Power Take-Off (PTO) mechanisms and d) three catenary mooring lines positioned at the three side columns of the semi-submersible. The combined concept with two rotating flaps and a semi-submersible platform is shown in Fig. 1. The origin of the coordinate system (XYZ) is placed at the still water level.

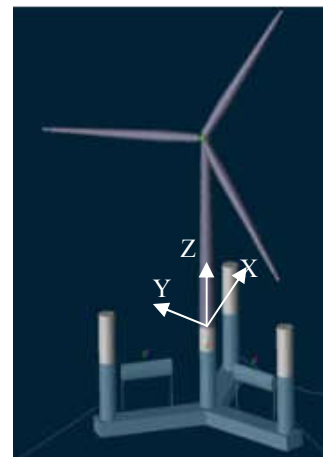


Figure 1. Semi-submersible wind turbine with two rotating flaps

The braceless semi-submersible platform is used. This concept is designed to support a 5 MW wind turbine in both operational and survival seas [4].

In the present study, the wind turbine corresponds to the NREL 5 MW reference wind turbine [20] with the OC3 Hywind wind tower [21]. The tower of the wind turbine starts 10 m above the waterline. Basic design characteristics of the different

parts of the combined concept are tabulated in Table 1 as well as in [4] and [22].

The wave energy converter is a fully submerged rotating flap; the upper point of the flap in its mean position is 2 m below the still water level and the lower point of the flap is 15 m above the pontoon of the semi-submersible platform. The cross section of each flap has an elliptical shape with major axis equal to 7 m and minor axis equal to 3.5 m. The major axis of the flap has direction that coincides with the direction of the vertical Z axis of the global coordinate system. The length, L_F , of each flap is 20 m. Each flap is connected with the pontoons of the semi-submersible through two rigid structural arms at the flap's two edges. Each arm is rigidly connected with the flap at the higher ends as well as is connected at the lower ends with a PTO mechanism with constant damping coefficient value with respect to the rotational motion of the flap. The PTO mechanism is rigidly connected with the pontoon of the semi-submersible platform.

Three catenary mooring lines are used for the station keeping of the semi-submersible platform and are positioned in a way such that the angle in between the mooring lines is 120 degrees. More details with regard to the numerical modeling of the wave energy converter as well as detailed description of the geometry and the characteristics of the combined semi-submersible with rotating flaps can be found in [22].

Table 1. Design characteristics of the combined concept

Property	Value
Draft [m]	30
Displacement of semi-submersible platform [t]	10,555
Length of the flap[m]	20
Height of the flap [m]	7
Distance of the inner edge of the flap from central column [m]	15
Mass of each flap (distributed uniformly to its area) [kg]	100,000.0
Displacement of each flap [t]	394.47
PTO Damping coefficient [N*m*sec/deg]	650,000

Three different cases are examined and their responses are compared; the first one is the case that the semi-submersible support-platform does not contain any wave energy device and operates as pure floating wind turbine and named hereafter as SWT, the second one is the case that two rotating flaps (Fig. 1) are placed at the pontoons of the semi-submersible support-platform and named hereafter as SFC₁ and the third case is the one that three rotating flaps are placed at the pontoons of the semi-submersible support-platform and named hereafter as SFC₂. It should be stressed that ballast water is adjusted for the cases with two or three rotating flaps in order to keep the draft value to be the same as is for the SWT case. A plane view of the combined concept SFC₂ that contains three rotating flaps namely the WEC₁, WEC₂ and WEC₃ is shown in Fig. 2. It is

noted that the SFC₁ contains only two rotating flaps namely the WEC₂ and WEC₃. In the same figure ML₁, ML₂ and ML₃ symbolize the three catenary mooring lines.

As far as the wind and wave environmental conditions are concerned EC_i, $i = 1 \sim 6$, the Site no. 14 of the MARINA platform project was selected [23]. Site 14 is in the northern North Sea, off the Norwegian coast and has water depth of 200 m. All the examined EC_i, $i = 1 \sim 6$, represent a range of possible expected operational conditions for given hub-height mean wind speed, U_w . The examined conditions EC_i, $i = 1 \sim 6$, are presented in Table 2. H_s is the significant wave height and T_p is the peak period of the JONSWAP spectrum that is used in order to simulate irregular waves. For all the examined spectra the peakedness factor is considered equal to 3.3. Both wind and wave are considered aligned with mean direction that is parallel to the X axis ($\beta=0^\circ$) (Fig. 2). In total six one-hour (3,600 sec) simulations are examined in the present study. It is noted that the overall simulation time for each EC_i is 4,100 sec; the first 500 sec have not been considered.

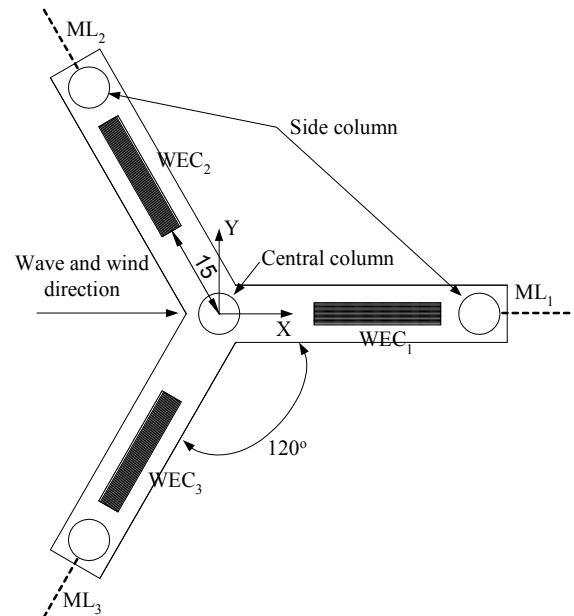


Figure 2. Plane view of the examined combined concept SFC₂ with mooring lines ML_i, $i=1, 2$ and 3

Table 2. Environmental conditions EC_i, $i = 1 \sim 6$

EC _i	U_w (m/sec)	H_s (m)	T_p (sec)
EC ₁	11.4	2.4	10.1
EC ₂	11.4	3.5	10.5
EC ₃	11.4	4.4	11.1
EC ₄	18.0	3.8	11.0
EC ₅	18.0	4.9	11.4
EC ₆	18.0	6.4	11.9

The fully coupled numerical analyses of the combined concept in the time-domain in both wind and wave environmental conditions EC_i , $i=1 \sim 6$, are carried out using the coupled numerical analysis tool Simo/Riflex/AeroDyn ([19]), which was developed by Marintek [24] and Centre for Ships and Ocean Structures (CeSOS) in Trondheim, Norway.

This tool further extends the capabilities of the Simo [25], Riflex [26] and AeroDyn [27] tools. A detailed description of the modeling and the numerical model of SFC₂, and more specifically the combined concept of semi-submersible wind turbine with three rotating flaps, is presented in [22].

RESULTS AND DISCUSSION

The effect of the utilizing two or three rotating flaps on the semi-submersible platform's response, namely, stability parameters, rigid body motions in six degrees of freedom of the semi-submersible platform, tension of the mooring lines at the fairlead, internal loads of tower and blades and aggregate produced power is analyzed next.

Influence of the rotating flaps on the stability parameters

Initially, stability analysis was performed for the three different examined cases, SWT, SFC₁ and SFC₂ considering the maximum steady wind turbine loads at rated wind speed. For all the three cases ballast water mass is utilized. The required water ballast mass is placed at the available empty space inside the pontoons and at the available empty space inside the three side columns of the semi-submersible platform. The stability analysis was performed with the HydroD software of the DNV SESAM package [28]. In order to have the rotating flaps fully submerged and connected with the semi-submersible platform an additional ballast water mass of 287 tonnes for each flap is required. In order to have the SFC₁ and the SFC₂ with the same draft as SWT, the ballast water of SFC₁ and SFC₂ has been recalculated. It is noted that since the pontoons are already filled with water the additional ballast mass is placed in the three side columns.

The operation of the rotating flaps and consequently the increase of the required ballast mass have as an effect the shifting of both the centre of gravity (CoG) and the centre of buoyancy (CoB) to higher level (Table 3) since the additional required ballast mass is placed in the side columns of the semi-submersible platform. Moreover, the operation of the flaps results in the increase of the absolute value of the metacentric height. Between SFC₁ and SFC₂ very small differences are obtained regarding the value of the metacentric height. In Figure 3 the righting moment curve as calculated from the stability analysis is presented. All the three curves present the same pattern. For positive heel angles the SFC₁ and the SFC₂ obtain almost the same righting moment values, for specific heel angle, that are larger compared to the values obtained for the case of SWT. For negative heel angles the SFC₁ has very close values with the ones that correspond to the SWT case.

The righting moment curve for the SFC₂ is sharper than those for SWT and SFC₁.

Table 3. Stability analysis results

Variable	SWT	SFC ₁	SFC ₂
Ballast mass [tonnes]	7,934.36	8,525.04	8,820.38
Metacentric height [m]	4.46	4.56	4.52
Heeling-righting moment intercept [deg]	8.86	8.26	7.87
Z _{CoG} [m]	-18.87	-18.33	-18.02
Z _{CoB} [m]	-22.43	-21.27	-20.74

In order to examine the stability of the semi-submersible platform with a specific inclining moment a threshold related to the heeling moment is considered; the threshold is defined to be equal to ± 74 MNm which is equal to the maximum induced heeling moment due to the wind turbine steady force at rated wind speed. The operation of the flaps has as a result the gradually decrease of the angle that corresponds to the first interception between the righting moment and the heeling moment. For positive heel angle this interception angle from 8.86 deg that corresponds to the case of SWT, decreases to 8.26 deg that corresponds to SFC₁, and finally decreases to 7.87 deg that corresponds to SFC₂. Based on the righting moment curve SFC₁ and SFC₂ may get better stability compared to the SWT. For negative heel angle this interception angle from -8.8 deg that corresponds to the case of SWT, increases to -8.2 deg that corresponds to SFC₁, and finally increases to -7.1 deg that corresponds to SFC₂. However, it should be noted that the stability analysis is performed considering that the rotating flaps are rigidly connected with the semi-submersible platform.

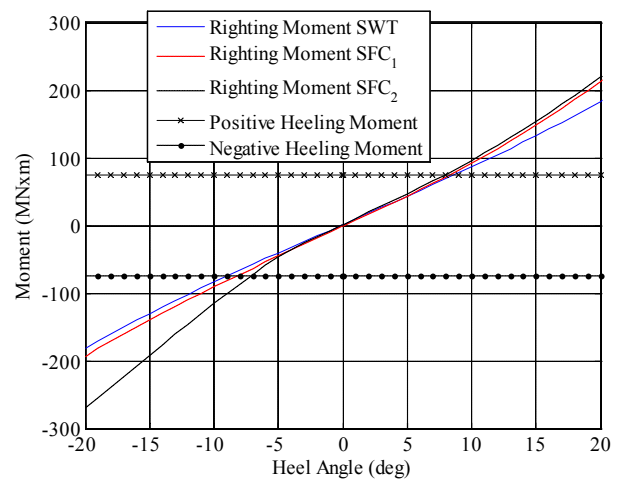


Figure 3. Righting moment curve (wind direction of 0°)

Simulation of decay tests

Numerical analyses of decay tests have been carried out to determine the natural periods of the six degrees of freedom for rigid body motions of the semi-submersible namely, surge, sway, heave, roll, pitch and yaw. The normalized natural periods are tabulated in Table 4 for SFC₁ and SFC₂. The normalized periods have been calculated with respect to the periods of the SWT.

Table 4. Normalized natural periods as calculated by decay tests for SFC₁ and SFC₂

Degree of freedom	SFC ₁	SFC ₂
Surge, ξ_1	1.0514	1.0665
Sway, ξ_2	1.0269	1.0224
Heave, ξ_3	1.0257	1.0432
Roll, ξ_4	0.9926	0.9842
Pitch, ξ_5	1.0137	1.0166
Yaw, ξ_6	1.0573	1.0865

The combined operation of the rotating flaps has a very small effect on the natural periods of the semi-submersible platform. The small differences result mainly from the water ballast mass that is different between the three examined cases. SFC₁ and SFC₂ have natural periods that are slightly different in all six rigid body degrees of freedom. It is mentioned that for the calculation of the natural periods of SFC₁ and SFC₂ the rotating flaps are connected with the semi-submersible platform with PTO mechanisms with characteristics as mentioned in Table 1.

Influence of the rotating flaps on the motions of the semi-submersible platform in turbulent wind and random seas

The effect of the combined operation of two or three rotating flaps on the semi-submersible platform's motions is discussed below. It should be noted that in the presented results μ denotes the mean value of the corresponding response quantity, σ denotes the standard deviation and max denotes the maximum value that the response quantity obtains in a time period of the one hour simulation for each EC_i, $i = 1 \sim 6$. In Table 5 the σ and max values of the motions in six rigid degrees of freedom for the SWT and for each EC_i, $i = 1 \sim 6$ are presented. Each max of the ξ_1 and of the ξ_5 is presented for EC₃ while each max of the ξ_2 and of the ξ_6 is presented for EC₁. In Figure 4 bar plots of the relative difference, ε , for the max values of the six rigid body degrees are presented; in Figure 4a the ε values are calculated by the comparison between the SWT and the SFC₁ while in Figure 4b the bar plots of the ε correspond to those as calculated between the SWT and the SFC₂. The relative difference, ε , for specific response quantity is defined as the quotient of the subtraction between the value that this response has for the combined concept, SFC₁ or SFC₂,

with the value that this response has for the case of SWT divided by the value that this response has for the case of SWT and is expressed in percent.

Table 5. Standard deviation, σ , and max values of the motions in six rigid degrees of freedom for EC_i, $i = 1 \sim 6$ for the SWT concept

	EC ₁	EC ₂	EC ₃	EC ₄	EC ₅	EC ₆
σ_{ξ_1} (m)	0.984	0.961	0.960	0.522	0.579	0.705
max $_{\xi_1}$ (m)	9.181	9.379	9.621	5.373	5.465	5.887
σ_{ξ_2} (m)	0.267	0.237	0.217	0.209	0.191	0.173
max $_{\xi_2}$ (m)	0.626	0.545	0.506	0.445	0.390	0.308
σ_{ξ_3} (m)	0.132	0.206	0.292	0.249	0.344	0.487
max $_{\xi_3}$ (m)	0.385	0.654	0.989	0.872	1.155	1.629
σ_{ξ_4} (deg)	0.278	0.244	0.224	0.342	0.316	0.290
max $_{\xi_4}$ (deg)	1.303	1.202	1.142	1.502	1.501	1.520
σ_{ξ_5} (deg)	0.963	0.960	0.954	0.707	0.700	0.700
max $_{\xi_5}$ (deg)	8.342	8.401	8.545	6.052	5.906	5.716
σ_{ξ_6} (deg)	0.684	0.651	0.629	0.897	0.842	0.782
max $_{\xi_6}$ (deg)	2.159	8.401	1.934	2.09	1.898	1.807

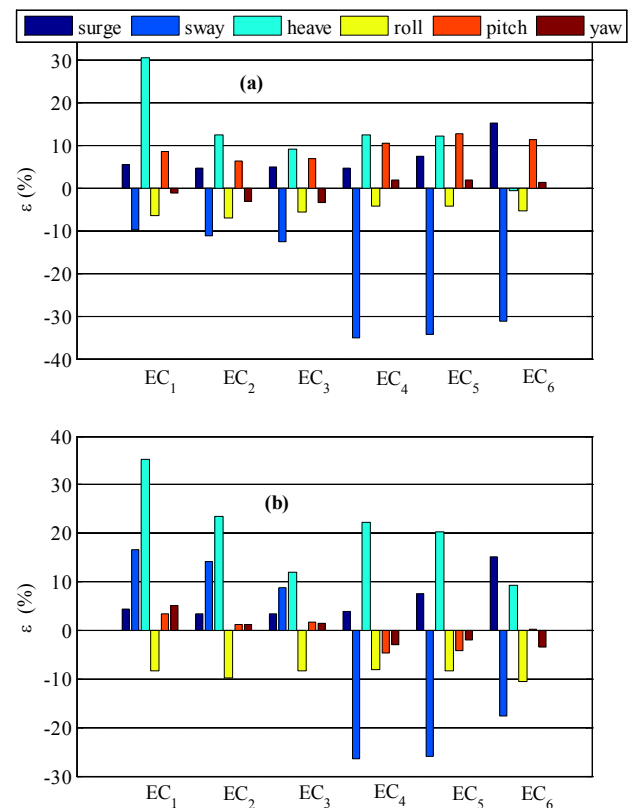


Figure 4. Bar plots of ε of motions' max values for SFC₁ (Fig. 4a) and for SFC₂ (Fig. 4b)

With regard to the surge motion, the SFC₁ and SFC₂ have larger max value of the surge motions for all the examined EC_i, *i*= 1 ~ 6. For the case of SFC₁ (Fig. 4a) the calculated ε values are between 4.62% and 15.17%; while for the case of SFC₂ the calculated ε values are in a range between 3.33% and 15.07%. Regarding the sway motion, the operation of the two rotating flaps, and consequently for the SFC₁ case, results to a significant decrease of the max ξ_2 value. The calculated ε obtains values between 9.98% and 35.14% for EC₁ and EC₄ respectively. Contrary to the SFC₁, and for U_w=11.4 m/sec the operation of three rotating flaps, SFC₂ case, has as a result the increase of the max sway motion of the platform up to a level of 16.70%. The presence of the small non zero values of sway, roll and yaw are due to the existence of the wind turbine loads. Compared to the other five motions the heave motion is the most affected. The operation of the rotating flaps has as an effect the increase of the heave max value up to 35.23% for EC₁ and SFC₂ case. For the heave motion and compared to SFC₁, SFC₂ obtains larger ε values for all the examined EC_i, *i*= 1 ~ 6. With regard to the roll of the semi-submersible platform, the operation of the rotating flaps has as a result the decrease of the max value of this response for both combined concepts SFC₁ and SFC₂. As far as the pitch degree of freedom, for the case of SFC₁ the ε values that are obtained are between 6.33% and 12.56%. For SFC₂ the ε of the max values of the pitch motion is limited to an upper level of 3.44% for EC₄. In Figure 5 the time history of the pitch motion, ξ_5 , of the semi-submersible platform for SFC₁ and EC₅ is presented. For EC₅ the pitch obtains its maximum value compared to all the examined EC_i, *i*= 1 ~ 6. The maximum value of the ξ_5 is 6.648 deg. It is found that the yaw motion is less affected than the other degrees of freedom. The introduction of the rotating flaps increases the max ξ_6 value up to 5.04% for SFC₂ and EC₁.

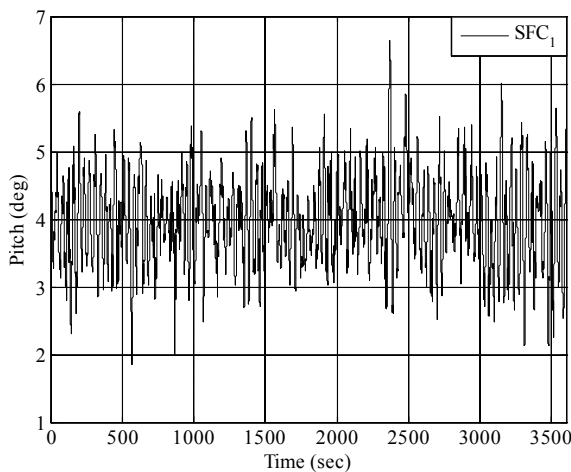


Figure 5. Time history of pitch motion, ξ_5 , of the semi-submersible platform for SFC₁ and EC₅

Influence of the rotating flaps on the mooring line tension

In Table 6 the μ , σ and max values of the mooring line tension, TML_k, *k*=1 and 2, for the case of SWT for EC_i, *i*= 1 ~ 6 are presented. Due to the geometry that the mooring lines have and wave and wind load direction the mooring lines ML₂ and ML₃ have tension values that are very close. The ML₂ and ML₃ are the most heavily loaded mooring lines of the SWT.

In Figure 6 bar plots of the calculated ε values of the max tensions values TML₁ and TML₂ are presented for all the examined EC_i, *i*= 1 ~ 6. In general, the introduction of the rotating flaps does not result in significant differences for the mooring line tensions. For the environmental conditions EC_i, *i*= 1, 2, 3, 4 and 5, the ε is smaller than 2%. Regarding to the mooring lines ML₁ and ML₂ of both the SFC₁ and SFC₂ for EC₆, the operation of the rotating flaps results in an increase of the max_{TML2} up to 5.1% and 5.4% respectively. In Figure 7 time histories of the TML₂ for the examined SWT, SFC₁ and SFC₂ for EC₆ are shown

Table 6. Mean value, μ , standard deviation, σ , and max values of the tensions, TML_k, *k*=1 and 2, of ML₁ and ML₂ for EC_i, *i*= 1 ~ 6 for SWT concept

	EC ₁	EC ₂	EC ₃	EC ₄	EC ₅	EC ₆
μ_{TML1} (kN)	1338	1335	1334	1469	1467	1463
σ_{TML1} (kN)	77.88	75.47	74.49	65.38	68.8	80.92
max _{TML1} (kN)	1617	1613	1622	1733	1751	1824
μ_{TML2} (kN)	1931	1933	1934	1825	1826	1829
σ_{TML2} (kN)	52.47	53.67	56.10	42.11	47.43	59.71
max _{TML2} (kN)	2138	2155	2165	1994	2026	2107

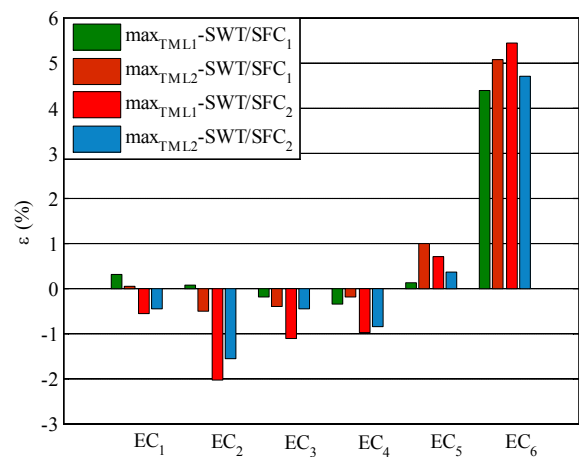


Figure 6. Bar plots of ε of the max mooring lines tension TML₁ and TML₂ for EC_i, *i*= 1 ~ 6

Influence of the rotating flaps on the forces in the tower and blade

The effect of the introducing two or three rotating flaps on the fore-aft bending moment, M_y , of the tower at two different positions as well as on the bending moment, $M_{y,bl}$, of one blade is examined and reported. The tower bending moment is calculated at: (a) the base of the tower with bending moment, $M_{y,tb}$, and (b) the middle of the height of the tower with bending moment, $M_{y,tc}$.

In Table 7 the μ and σ values of the $M_{y,tb}$, $M_{y,tc}$ and $M_{y,bl}$ for all the examined EC_i , $i=1 \sim 6$ are presented. The values of $M_{y,tb}$ are larger than those of $M_{y,tc}$. The $M_{y,tb}$, $M_{y,tc}$ and $M_{y,bl}$ values are not affected by the H_s . For $U_w=11.4$ m/sec the values of $M_{y,tb}$, $M_{y,tc}$ and $M_{y,bl}$ have larger values compared to the corresponding values for $U_w=18.0$ m/sec.

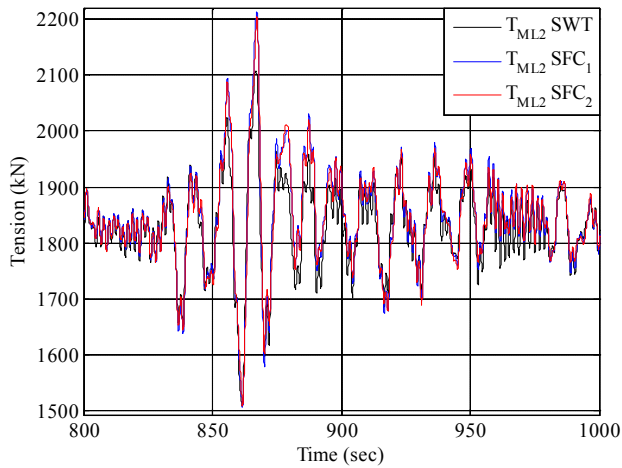


Figure 7. Time history of T_{ML2} for the examined SWT, SFC_1 and SFC_2 for EC_6

Table 7. Mean value, μ , and standard deviation, σ , of the $M_{y,tb}$, $M_{y,tc}$ and $M_{y,bl}$ of the SWT's tower and one blade for EC_i , $i=1 \sim 6$

Value	EC_1	EC_2	EC_3	EC_4	EC_5	EC_6
$\mu_{M_{y,tb}}$ (MNm)	86.92	86.96	86.97	50.95	50.97	51.01
$\sigma_{M_{y,tb}}$ (MNm)	13.86	14.20	14.36	11.63	12.07	12.78
$\mu_{M_{y,tc}}$ (MNm)	42.09	42.10	42.1	25.2	25.2	25.2
$\sigma_{M_{y,tc}}$ (MNm)	6.55	6.72	6.79	5.59	5.8	6.15
$\mu_{M_{y,bl}}$ (MNm)	9.04	9.04	9.038	4.73	4.73	4.71
$\sigma_{M_{y,bl}}$ (MNm)	1.67	1.67	1.67	1.98	1.98	1.99

In Figure 8 bar plots of the relative difference, ϵ , for the mean values of the $M_{y,tb}$, $M_{y,tc}$ and $M_{y,bl}$ are presented; in Figure 8a the ϵ values are calculated by the comparison between the SWT and the SFC_1 while in Figure 8b the bar plots of the ϵ correspond to those as calculated between the SWT and the SFC_2 . The introduction of two rotating flaps (Fig. 8a) increases the $M_{y,tb}$ and $M_{y,tc}$ for all the examined environmental conditions; the calculated ϵ values are in a range of 3.10% to 5.22%. Meanwhile, for the case of SFC_2 the calculated ϵ values are in a range of -0.47% to 0.78%. With regard to the $M_{y,bl}$ the calculated ϵ values for both SFC_1 and SFC_2 are very small with a maximum value of 0.6% for SFC_1 and EC_4 .

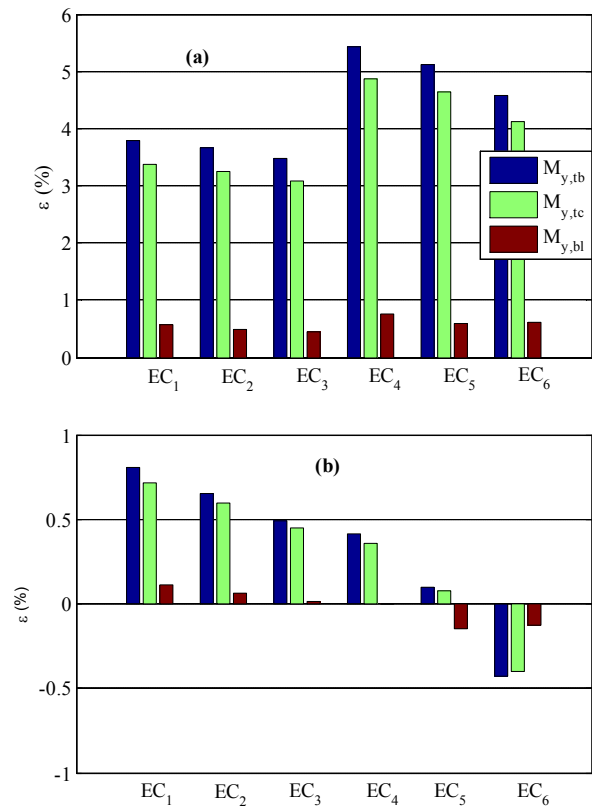


Figure 8. Bar plots of ϵ of mean value, μ , of the $M_{y,tb}$, $M_{y,tc}$ and $M_{y,bl}$ for SFC_1 (Fig. 8a) and for SFC_2 (Fig. 8b)

Influence of the rotating flaps on the produced power

The effect of the introducing two or three rotating flaps on the produced power by the wind turbine, on the produced power by the rotating flaps and on the total produced power is discussed below.

In Table 8 the μ and σ values of wind's turbine produced power, P_{WT} , for the examined cases SWT, SFC_1 and SFC_2 for EC_i , $i=1 \sim 6$ are presented. It is noted that the presented wind power values in Table 8 have been calculated with an efficiency factor equal to 94.4% which is representative for NREL 5MW wind turbine. In general, the introduction of WECs has a

negligible effect on both the calculated μ and σ of the produced wind power, P_{WT} .

Table 8. Mean value, μ , and standard deviation, σ , of the produced wind power, P_{WT} , for SWT, SFC₁ and SFC₂, and for EC_i, $i=1 \sim 6$

		EC ₁	EC ₂	EC ₃	EC ₄	EC ₅	EC ₆
SWT	μ_{PWT} (kW)	4,422	4,422	4,422	5,000	5,000	5,000
	σ_{PWT} (kW)	709.6	709.9	710.0	234.5	234.7	234.8
SFC ₁	μ_{PWT} (kW)	4,416	4,417	4,417	5,000	5,000	5,000
	σ_{PWT} (kW)	712.0	712.0	712.0	234.7	234.9	237.9
SFC ₂	μ_{PWT} (kW)	4,422	4,423	4,423	5,000	5,000	5,000
	σ_{PWT} (kW)	709.1	708.9	709.9	232.5	234.0	236.8

Table 9. Mean value, μ , and standard deviation, σ , of the total rotating flaps' produced power, P_{WEC} , for SFC₁ and SFC₂, and for EC_i, $i=1 \sim 6$

EC _i $i=1 \sim 6$	SFC ₁		SFC ₂	
	$\mu_{P_{WEC}}$ (kW)	$\max_{P_{WEC}}$ (kW)	$\mu_{P_{WEC}}$ (kW)	$\max_{P_{WEC}}$ (kW)
EC ₁	53.5	1,165.5	54.5	1,175
EC ₂	115.5	2,192.5	117	2,214.5
EC ₃	185.5	3,798	187.5	3,825.5
EC ₄	139.5	2,694	140.5	2,720.5
EC ₅	233	3,956	235	3,991
EC ₆	396	6,930	397.5	6,995

In Table 9 the mean (μ) and max values of the total produced power from the rotating flaps WEC₂ and WEC₃ for the SFC₁ and SFC₂ are presented for EC_i, $i=1 \sim 6$. It is noted that the presented produced power values in Table 9 have been calculated with an efficiency factor equal to 50%. It is noted that since the wave direction is parallel to the X axis the WEC₁ of the SFC₂ (Fig. 2) has limited rotational motion with respect to the global Y axis and as a result WEC₁ has almost zero wave energy production. SFC₁ and SFC₂ have very small differences with regard to the total produced power from the rotating flaps. For SFC₁ the total produced power from the rotating flaps varies between 53.5 kW and 396 kW while for the case of SFC₂ the total produced power from the rotating flaps varies between 54.5 kW and 397.5 kW. The produced power is not influenced by the mean wind speed, U_w . For all the examined EC_i, $i=1 \sim 6$ the instantaneous $\max_{P_{WEC}}$ is up to 21.5 times larger than the $\mu_{P_{WEC}}$. In Figure 9 a time history of the produced power of WEC₂ for SFC₁ and EC₂ is presented.

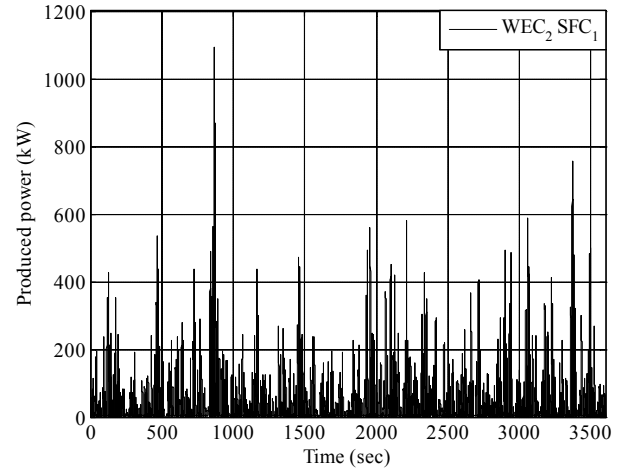


Figure 9. Time history of the produced power of the rotating flap WEC₂ for SFC₁ and EC₂

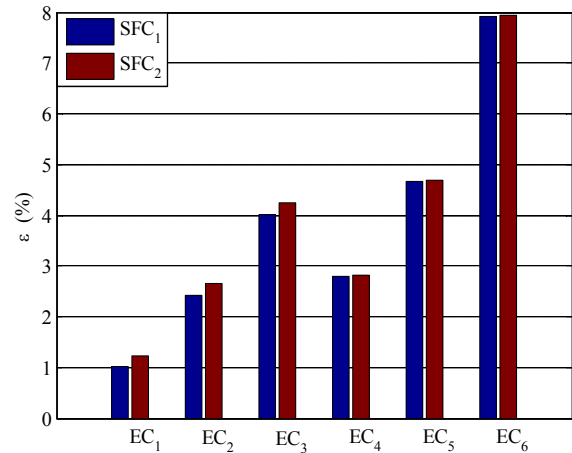


Figure 10. Bar plots of ϵ for the aggregate produced power for SFC₁ and SFC₂ and for EC_i, $i=1 \sim 6$

In Figure 10 bar plots of the relative difference, ϵ , for the aggregate produced power are presented for the combined concepts SFC₁ and SFC₂ and for environmental conditions EC_i, $i=1 \sim 6$. In all environmental conditions EC_i an increase of the produced power is presented. Particularly for aligned mean wind and wave direction the operation of the combined concepts SFC₁ and SFC₂ results to same level of increase of the produced power. For the case of SFC₁ the calculated ϵ values are between 1% and 7.9%; meanwhile for the case of SFC₂ the calculated ϵ values are in a range of 1.1% to 8%. As expected, the ϵ of the aggregate produced power is not influenced by the level of the mean wind speed. The larger ϵ values are obtained for environmental conditions with large H_s , namely for EC₃, EC₅ and EC₆. The combined operation of two rotating flaps, SFC₁, has as a result the increase of the produced power in a mean level of 3.8%, while the operation of three rotating flaps, SFC₂,

has as a result the increase of the produced power in a mean level of 3.9% for the six environmental conditions EC_i , $i=1 \sim 6$.

Influence of the incident wave direction on the produced power, P_{WEC} , by SFC_1 and SFC_2

The effect of the incident wave direction on the produced power, P_{WEC} , from SFC_1 and SFC_2 is discussed below. The case with mean wind direction $\beta=0^\circ$ and incident wave direction $\beta=90^\circ$ is examined.

In Figure 11 bar plots of the relative difference, ϵ_{WEC} , for the produced power, P_{WEC} , by the rotating flaps are shown and for environmental conditions EC_i , $i=1 \sim 6$. The relative difference, ϵ_{WEC} , for the produced power by the rotating flaps is defined as the quotient of the produced power of the combined concept SFC_2 divided by the value that the produced power has for the combined concept SFC_1 and is expressed in percent. In all environmental conditions EC_i , $i=1 \sim 6$, an increase of the produced power by the rotating flaps is presented for SFC_2 in a range of 125% to 132%. For incident wave direction different than $\beta=0^\circ$ and compared to SFC_1 the WEC_1 rotating flap of SFC_2 operates and produces power. In Figure 12 a comparison of the total produced power by the rotating flaps for SFC_1 and SFC_2 and for EC_2 is shown for mean wind direction $\beta=0^\circ$ and incident wave direction $\beta=90^\circ$.

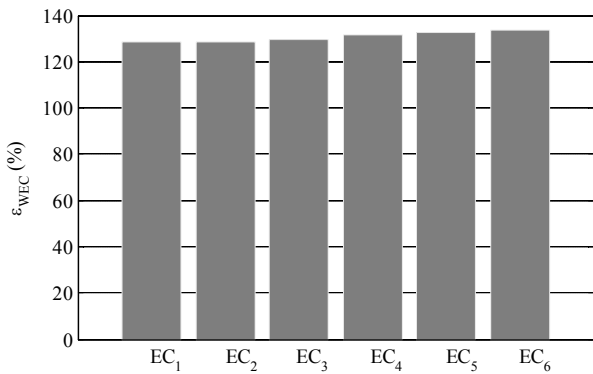


Figure 11. Bar plots of ϵ_{WEC} for the produced power P_{WEC} from the rotating flaps for EC_i , $i=1 \sim 6$ and incident wave direction $\beta=90^\circ$.

CONCLUSIONS

In the present paper the behavior of a combined three column semi-submersible wind turbine and rotating flap type wave energy converters hinged at the pontoons of the semi-submersible has been examined. Modeling and analysis in the time-domain of the combined concept in stochastic wind and wave environment are carried out using the coupled tool Simo/Riflex/AeroDyn. Analysis is performed in order to examine the effect of introducing two or three rotating flaps on the response of a floating semi submersible wind turbine.

The main conclusions are as follow:

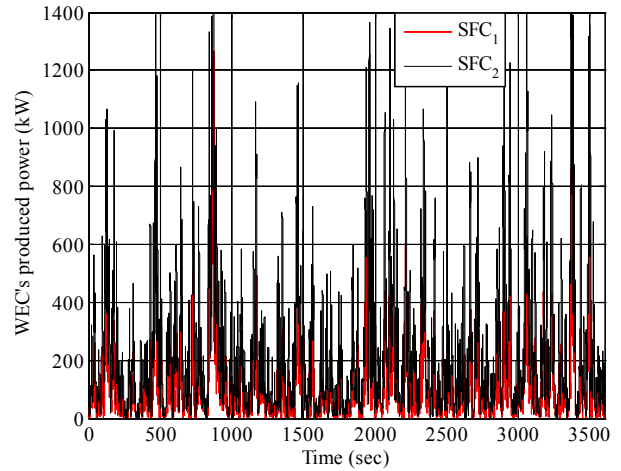


Figure 12. Time history of total WEC's produced power for EC_2 and for SFC_1 and SFC_2 .

- The natural periods of the semi-submersible platform are not much influenced by introducing the rotating flaps.
- The introduction of the rotating flaps results in a max increase of: (a) 5.4% of the mooring line tensions, (b) 5.6% of the tower's bending moment and (c) 0.8% of the blade's bending moment.
- The introduction of the rotating flaps doesn't affect the produced wind power.
- The total produced power is increased by 1% ~ 8% for the examined environmental conditions.
- For incident wave direction different than $\beta=0^\circ$ and compared to SFC_1 , SFC_2 obtains larger amount of produced power, P_{WEC} , by the rotating flaps.
- For $\beta=30^\circ$ and for the examined environmental conditions, an increase of the produced power by the rotating flaps is presented for SFC_2 compared to SFC_1 in a mean range of 129%.

Finally, it would be interesting to perform a long-term analysis reflecting the directionality of the waves in order to compare the annual average produced power of the combined concepts SFC_1 and SFC_2 with the corresponding annual average produced power of the pure semi-submersible wind turbine for selected sites.

ACKNOWLEDGMENTS

The authors acknowledge the financial support from the European Union Seventh Framework Programme theme FP7-ENERGY (MARINA Platform – Marine Renewable Integrated application Platform, Grant Agreement no. 241402). Chenyu Luan acknowledges the financial support from the Research Council of Norway granted through the Centre for Ships and Ocean Structures and the Norwegian Research Centre for Offshore Wind Technology (NOWITECH), NTNU as well.

REFERENCES

- [1] Jonkman, J. M. and Matha, D., (2011), "Dynamics of offshore floating wind turbines-analysis of three concepts", *Wind Energy*, 14:557–569.
- [2] Robertson, A., Jonkman J., Masciola, M., Song, H., Goupee, A., Coulling, A. and Luan C., (2012), "Definition of the Semisubmersible Floating System for Phase II of OC4", Offshore Code Comparison Collaboration Continuation (OC4) for IEA Task 30. Vancouver, Canada.
- [3] Luan, C., Gao, Z. and Moan, T., (2013), "Modelling analysis of a semi-submersible wind turbine with a central tower with emphasis on the brace system", in 32nd International Conference on Ocean, Offshore and Arctic Engineering, no.OMAE2013-10408, Nantes, France.
- [4] Luan, C., Gao, Z., and Moan, T., "Conceptual designs of a 5-MW and a 10-MW semi-submersible wind turbine with emphasis on the design procedure", *Journal of Offshore Mechanics and Arctic Engineering*, (submitted, 2014).
- [5] Falnes, J., (2007), "A review of wave-energy extraction", *Marine Structures*, 20:185–201.
- [6] Falcao, A., (2010), "Wave energy utilization: A review of the technologies", *Renewable and Sustainable Energy Reviews*, 14:899–918.
- [7] Caska, A. J. and Finnigan, T. D., (2008), "Hydrodynamic characteristics of a cylindrical bottom-pivoted wave energy absorber", *Ocean Engineering*, 35:6–16.
- [8] Renzi, E. and Dias, F., (2012), "Relations for a periodic array of flap-type wave energy converters", *Applied Ocean Research*, 39:31–39.
- [9] The Engineering Business Ltd, EB Frond wave energy converter – phase 2, Tech. rep., DTI (2005).
- [10] Kurniawan, A. and Moan, T., (2012), "Characteristics of a pitching wave absorber with rotatable flap", *Energy Procedia*, 20:134–147.
- [11] Kurniawan, A. and Moan, T., (2013), "Optimal geometries for wave absorbers oscillating about a fixed axis", *IEEE Journal of Oceanic Engineering*, 38:117–130.
- [12] MARINA PLATFORM, (Online) Available at: <http://www.marina-platform.info/index.aspx> [Accessed 29 December 2013].
- [13] Bachynski, E. E. and Moan, T., (2013), "Point Absorber Design for a Combined Wind and Wave Energy Converter on a Tension-Leg Support Structure", in 32nd International Conference on Ocean, Offshore and Arctic Engineering, no.OMAE2013-10429, Nantes, France.
- [14] Soulard, T., Babarit, A., Borgarino, B., Wyns, M. and Harismendy, M., (2013), "C-HYP: A combined wave and wind energy platform with balanced contributions", in 32nd International Conference on Ocean, Offshore and Arctic Engineering, no. OMAE2013-10778, Nantes, France.
- [15] Aubult, A., Alves, M., Sarmiento, A., Roddier, D. and Peiffer, A., (2011), "Modeling of an oscillating water column on the floating foundation WindFloat", in 30th International Conference on Ocean, Offshore and Arctic Engineering, no. OMAE2011-49014, Rotterdam, Netherland.
- [16] Muliawan, M. J., Karimirad, M. and Moan, T., (2013), "Dynamic response and power performance of a combined spar-type floating wind turbine and coaxial floating wave energy converter", *Renewable Energy*, 50:47–57.
- [17] Muliawan, M. J., Karimirad, M., Gao, Z. and Moan, T., (2013), "Extreme Responses of a Combined Spar-Type Floating Wind Turbine and Floating Wave Energy Converter (STC) System with Survival Modes.", *Ocean Engineering*, 65:71–82.
- [18] Muliawan, M. J., Gao, Z., Moan, T. and Babarit, A. (2013), "Analysis of a Two-Body Floating Wave Energy Converter with Particular Focus on the Effects of Power Take-Off and Mooring Systems on Energy Capture", *Journal of Offshore Mechanics and Arctic Engineering*, 135 (3): 031902. doi:10.1115/1.4023796
- [19] Ormberg, H. and Bachynski, E.E., (2012), "Global analysis of floating wind turbines: Code development, model sensitivity and benchmark study", in The 22nd International Ocean and Polar Engineering Conference 2012: Rhodes, Greece.
- [20] Jonkman, J., Butterfield, S., Musial, W. and Scott, G., (2009), "Definition of a 5-MW Reference Wind Turbine for Offshore System Development", NREL/TP-500-38060, National Renewable Energy Laboratory, Golden, CO, U.S.A.
- [21] Jonkman J., (2010), "Definition of the Floating System for Phase IV of OC3", NREL/TP-500-47535, National Renewable Energy Laboratory, Golden, CO, USA.
- [22] Luan, C., Michailides, C., Gao, Z. and Moan, T., (2014), "Modeling and analysis of a 5 MW semi-submersible wind turbine combined with three flap-type Wave Energy Converters", in 33rd International Conference on Ocean, Offshore and Arctic Engineering, no.OMAE2014-24215, San Francisco, USA.
- [23] Lin, L., Gao, Z. and Moan, T., (2013), "Joint Environmental Data at Five European offshore sites for Design of Combined Wind and Wave Energy Devices", in 32nd International Conference on Ocean, Offshore and Arctic Engineering, no.OMAE2013-10156, Nantes, France.
- [24] Norwegian Marine Technology Research Institute (MARINTEK), (Online) Available at: <http://www.sintef.no/home/MARINTEK/> [Accessed 29 December 2013].
- [25] MARINTEK, 2011. SIMO User's Manual.
- [26] MARINTEK, 2011. RIFLEX User's Manual.
- [27] Moriarty P. J. and Hansen, A. C., 2005. AeroDyn theory manual. Tech. Rep. NREL/TP-500-36881.
- [28] DNV (Det Norske Veritas) software SESAM, Norway, HydroD, V4.0-10, build date 1 September 2008.